Proceedings of the Korean Nuclear Society Spring Meeting
Gwangju, Korea, May 2002

Experimental Simulation of SG Tubesheet Crevice Chemistry

Chi Bum Bahn, Si Hyoung Oh, Byung Gi Park, and Il Soon Hwang

Department of Nuclear Engineering, Seoul National University
San 56-1, Shinlim-dong, Gwanak-gu, Seoul 151-742, Korea

In Hyoung Rhee

Department of Chemical Engineering, Soonchunhyang University
San 53-1, Shinchang-myoun, Asan, Chungcheongnam-do 336-745, Korea

Uh Chul Kim, Jung Won Na

Korea Atomic Energy Research Institute
150 Dukjin-dong, Yusong-gu, Daejon 305-353, Korea

ABSTRACT

In a locally restricted geometry on the secondary side of steam generator (SG) in a pressurized water reactor (PWR), impurities in bulk water can be concentrated by boiling process to extreme pH that may then accelerate the corrosion of tubing and adjacent materials. To simulate a real SG tubesheet crevice, a high temperature/high pressure (HT/HP) crevice simulation system was constructed. Primary water was pumped at a high flow rate through a 3/4” outer-diameter tubing and a crevice section was made on the outer diameter (OD) side of the tubing. The simulated crevice area was monitored with thermocouples and electrodes for the measurement of temperature and electrochemical corrosion potential (ECP), respectively, in the crevice as well as free span. A secondary solution composed of 50 ppm Na and 200 ppb hydrogen (H_2) was supplied at a flow rate of about 4 L/hr. In an open tubesheet crevice with 0.15 mm radial gap and 40 mm depth, axial distributions of temperature and ECP were measured as a function of time and available superheat. Sodium hydroxide (NaOH) concentration process in the crevice and the resultant evolution of crevice boiling regions were characterized from temperature and ECP data. Measured data for an open crevice showed a similar behavior to predictions by a thermodynamic equilibrium code. Magnetite-packed crevice had much longer time to reach a steady state than open crevice.

1. INTRODUCTION

In a PWR, SG tubings are made of alloy 600 (UNS N06600) or 690 (UNS N06690) and

steam is produced on the OD side. SG reliability has been one of the important issues encountered during PWR operations. Various corrosion phenomena in the SG were observed in the past [1]. In a locally restricted geometry on the OD side, trace impurities in the bulk water can be concentrated by boiling processes to extreme pH. SG tube degradation phenomena result from the concentration of impurities mainly at three locations: the tube support plate (TSP) crevice, the tubesheet crevice, and sludge/tubing crevice. These locations with concentrated solutions may then develop OD stress corrosion cracking/inter-granular attack (ODSCC/IGA) that is the one of the principal degradation mechanisms in recent years [2]. To mitigate the ODSCC/IGA in the restricted geometries and to improve SG integrity, the detailed understanding of boiling crevice behaviors is needed.

A near-neutral crevice is the environment likely to produce the lowest SCC/IGA crack growth rate [3]. Based on this fact, the EPRI has developed the molar ratio control (MRC) program, of which the goal is to maintain the crevice pH nominally in the pH range between 5 and 9 at the operating temperature [4]. During a plant operation, however, the SG the crevice conditions cannot be directly monitored due to difficulty of instrumentations at real crevices. Hideout return test, an indirect way to estimate crevice pH, is conducted only once per fuel cycle. It is expected that crevice pH can be varied with relatively short time constant in the case of contaminated secondary water chemistry [5]. Therefore real-time crevice monitoring methods need to be developed.

Baum [6] reviewed, in detail, the thermal-hydraulic and chemical phenomena in restricted regions and the free span area. Early crevice experiments were primarily focused on the characterization of thermal-hydraulic nature. Chemical and/or electrochemical measurements for crevices were conducted more recently. Kozawa and Aoki [7] investigated experimentally several boiling characteristics of a crevice between tube and tubesheet. A flat crevice and a fluid heating method were adopted. Their results showed that three regions of different boiling configurations could develop in a crevice; namely a region of a periodic water penetration and discharge region, a region of water droplets, and a steam-blanketing region. Visual observations of boiling process within the crevice between tube and TSP were conducted at high pressure [8]. The results confirmed the existence of three confinement-dependent boiling regions.

Baum and Curlee [9] performed tests in which the geometric, thermal, and hydraulic environments found between the tube and the TSP in typical PWR U-tube SG's were simulated. It was found that certain tube support configurations could produce a local liquid-deficient heat transfer regime which, in turn, could permit significant chemical concentration. The interrelationship between the heat and the mass transfer processes in the crevice geometry was further demonstrated by results of an analytic model. Sodium hideout studies in SG crevices were carried out systematically by Campan and Shoemaker [10]. A method using Na^{24} as a tracer was developed.

A technique was developed to study electrochemical phenomena in crevices that simulate the geometry in nuclear SG's. ECP was measured in TSP crevice geometry by Hermer et al. [11]. Lumsden et al. [5] constructed a system that simulated TSP crevice conditions. Experimental results agreed well with MULTEQ® predictions on the average boiling point elevation in the crevice, the analysis of the extracted crevice solutions, and the redox potential in the crevice and free span, once steady state conditions were attained. An electrochemical noise monitoring technique was evaluated in a refreshed autoclave system as a crevice

corrosion monitoring system for SG's [12].

An on-site model boiler facility was constructed by Kansai Electric Power Company at Ohi Unit 1 at the beginning of 1986 [13]. ECP monitoring in the blowdown water and pH monitoring in simulated SG crevices were carried out using the model boiler [13]. By analyzing directly sampled concentrated solution from a heated crevice of the model boiler, SG crevice environment was estimated [14,15].

To complement earlier work, the objectives of this study are set to develop a HT/HP SG crevice simulation system and to advance fundamental understanding of crevice concentration behavior. Also this work can lead to the development of an on-site SG monitor. A top-open circular crevice was designed to represent a tubesheet crevice.

2. EXPERIMENTAL

In an earlier work of the present authors, electric heater was used to simulate primary heating condition. But the heating method caused difficulties in simulating real SG crevice temperature distribution such as the local variation of surface heat flux and temperature rise with elevation. As the impact of these deviations on the simulation of tubesheet crevice is unknown at this time, a HT/HP crevice simulation system was chosen in this study. The system was composed of two main loops: a primary water loop and secondary water loop with a crevice. The primary water was circulated at a high flow rate of about 2,300 L/hr by a HT/HP centrifugal pump into a 3/4" OD 316 stainless steel (SS) tube. A 3.8 L autoclave was used as the primary water heater with the maximum power of 4.8 kW. High purity water deaerated with 5% hydrogen gas (nitrogen bal.) was charged by a diaphragm pressure pump and ejected through a back pressure regulator at about 2 L/hr. Primary pressure was maintained at 14.0 MPa with maximum 0.2 MPa fluctuation. In Fig. 1, the SG simulation vessel of the secondary side is schematically described. The vessel was made of 316 SS. To protect vessel from caustic stress corrosion cracking, electroless Ni plating with 10 μm thickness was applied on the whole vessel inner surfaces. To form a bottom-closed crevice the secondary vessel was machined to have a slightly over-sized crevice to the SS tube. Then thick electrolytic Ni plating was applied on 3/4" OD SS tube over the 40 mm long crevice section, and the plated section was finally machined to a radial crevice gap size of 0.15 mm. The secondary water storage tank, made of Ti, was also deaerated with 5% hydrogen gas (nitrogen bal.). The secondary water containing 50 ppm Na and 0.2 ppm H_2 was charged by a diaphragm pump and ejected through a back pressure regulator, as shown in Fig. 1. The dissolved hydrogen concentration is expected to have the same reducing power as hydrazine (H_2NNH_2) at about 300 ppb concentration. Flow rate of the secondary system was maintained at 4 L/hr. The secondary pressure was adjusted automatically by a PID-controlled back pressure regulator at 5.50 MPa with maximum 0.04 MPa fluctuation and the corresponding saturation temperature was 270 ^{o}C.

The crevice simulation vessel was instrumented with small size sensors including thermocouples and reference electrodes for the measurement of temperature and ECP distributions. Fig. 1 illustrates the locations of sensors installed in the crevice and the bulk regions, including two thermocouples in the bulk region and five thermocouples at crevice region. Primary inlet and outlet temperatures were monitored by separate sensors. All the

thermocouples were calibrated with the maximum temperature error of 1.2 ^{o}C.

Ag/AgCl external reference electrodes with high purity water as filling solution were used and two Pt electrodes were installed [16]. Prior to experiments, Ag/AgCl water-filled electrodes were calibrated as a function of temperature and were verified for their long-term stability. The maximum error of reference electrode potential is 20 mV. In both crevice and bulk regions, Ag/AgCl and Pt electrodes had the same axial location. In a tubesheet crevice with 0.15 mm gap and 40 mm depth, axial temperature distribution and Pt potential vs. Ag/AgCl water-filled electrode were measured with time. Under the assumption that Ni electrode would serve as hydrogen electrode in the reducing environment, the Ni-plated autoclave body potential vs. Ag/AgCl water-filled was also measured. Temperature and ECP data were measured by a Hewlett Packard (HP) Model 34401A multimeter through a HP Model 3495A multiplexer.

3. RESULTS & DISCCUSSIONS

Open Crevice

'Open Crevice' means that the crevice is empty and there is no impurity or particle at an initial state. Fig. 2 shows the axial temperature profiles at steady states for a range of primary water temperature. The vertical axis represents elevation from the top of crevice normalized by the crevice depth. The difference between the primary water temperature and the secondary saturation temperature represents available superheat, ΔT, for the crevice. As ΔT increased, the temperature gradient increased in the crevice, accompanied with elevation in bulk temperature. When the primary temperature equaled to 300 ^{o}C, the temperature of bulk region exceeded the saturation temperature. It was caused by the loop characteristics that the secondary water flow rate was not enough to maintain a subcooled condition in the free span region. Therefore the temperature data no longer represent crevice concentration behavior at such high primary temperature. Measurements using two different secondary autoclaves were shown to agree well with each other and hence data reproducibility for the crevice system was confirmed.

The secondary pressure was initially maintained at a value exceeding the saturation pressure until the primary temperature reached a steady state. Then, the secondary pressure was suddenly dropped to 5.50 MPa so that boiling could occur in the crevice. Fig. 3 shows the temperature measurement results as a function of time at ΔT=25 ^{o}C. As shown in Fig. 3, the temperature reached a steady state in about 10 hours after the first boiling occurred. The difference between the primary inlet temperature and the outlet temperature, ΔT_p, showed no significant change with time from a typical value of 1.0 ^{o}C. When the boiling was suppressed by increasing the secondary pressure, the temperature returned to the initial value. As described in Fig. 1, 'TC#1' represents the shallowest position and 'TC#5' represents the deepest position into the crevice from the zero level. It was found that from the shape of temperature variation the crevice region could be divided into two regions with different behaviors. One was the upper region including 'TC#1', 'TC#2', and 'TC#3' and the other was the lower region including 'TC#4' and 'TC#5'. Based on the earlier work, it was concluded that the upper region showed a wet or wet-and-dry behavior and the lower region had the

dryout nature [6,7]. It means that liquid can penetrate only to the upper region. From the boiling point elevation data, the crevice concentration factor for the open tubesheet crevice was estimated as about 1,000 for $\Delta T=25\ ^{o}C$ in the case of 50 ppm Na solution in the bulk.

Fig. 4 shows temperature and ECP measurement results as a function of time under the same condition as in Fig. 3. Before the boiling, the bulk and crevice ECP maintained at the same values of about -820 mV_{SHE}. With the boiling, bulk ECP slightly decreased and crevice ECP showed fluctuation. Crevice ECP suddenly dropped and remained stable at -940 mV_{SHE}. It was interpreted that water saturation was increased and the crevice solution was concentrated by boiling process having led to the crevice wetting with an increase of solution pH which caused the sudden ECP stabilization and decrease. When the boiling was suppressed later, crevice ECP returned to the initial value with about 40 mV deviation. The cause of deviation in the potential recover is not identified. 'TC#3 (crevice)' represents the temperature located at the same level as Ag/AgCl water-filled electrode.

The wetting of crevice at the ECP measurement location was observed only at $\Delta T=25\ ^{o}C$ although the boiling point elevation increased with ΔT. At $\Delta T<25\ ^{o}C$, the mixing of crevice solutes with bulk water could have been too high to cause a complete dryout and subsequent wetting at the ECP measurement location. At $\Delta T=30\ ^{o}C$, the bulk boiling might have prevented any significant amount of downward mass transfer that was necessary to cause wetting. In order to examine the postulation, the behavior of bulk water penetration into the crevice needs to be understood.

To analyze the behavior analytically, a liquid penetration depth model was introduced [17]. The liquid penetration depth or wetted length could be obtained as Eq. (1).

$$L = \frac{c^2 h_{fg}}{2q''}\left[gs^3\left(\rho_f - \rho_v\right)\right]^{1/2}\left[\rho_v^{-1/4} + \rho_f^{-1/4}\right]^{-2} \quad (1)$$

where, c denotes a geometrical factor assumed a unit in this calculation and h_{fg} is heat of vaporization. g is the acceleration of gravity and s means a diametral crevice width. ρ_f and ρ_g denote the density of liquid and vapor, respectively. Heat flux, q" can be obtained as Eq. (2).

$$q'' = h\left(T_p - T_{sat}\right) \quad (2)$$

where, h denotes the overall heat transfer coefficient and the value was referenced from other work [18]. T_p and T_{sat} represent the primary water temperature and the secondary saturation temperature, respectively. Fig. 5 shows the liquid penetration depth prediction results as a function of primary water temperature. The region deeper than liquid penetration depth could be considered as dry region. At $\Delta T=25\ ^{o}C$, as shown in Fig. 3, the regions including 'TC #4' and 'TC #5' were considered as dry regions. But prediction results estimated the liquid penetration depth shallower than the measurement results at $\Delta T=25\ ^{o}C$. This was probably because the referenced value of the overall heat transfer coefficient, h could not represent the experimental condition exactly. However, it was found from the simple model results that as ΔT increased, the dry region was spread out from the bottom of crevice. As illustrated schematically in Fig. 6, the boiling point elevation and resultant wetting behavior were varied

as a function of primary water temperature. At low ΔT, liquid could penetrate into the bottom of crevice and the mixing between bulk and crevice prevent mass concentration. As ΔT increased, the dry region occurred at the bottom of crevice and expanded. At the middle of crevice, the location of ECP measurement, vigorous liquid and vapor motions made difficult to get a meaningful ECP signal. But at higher ΔT, the concentrated liquid droplets were located in the middle of crevice and it became possible to get an ECP signal. In the earlier work of the present authors [19] and Baum's results [9], the concentration processes mainly occurred at the boundary between liquid penetration region and dryout region. Therefore, at ΔT=25 ^{o}C, it was concluded that the ECP location was included to the vapor and droplet region and the concentrated liquid droplet made a solid electric path enough to get a ECP signal.

By using MULTEQ-REDOX® Ver.2.22, high temperature solution pH, boiling point elevation, and oxidation-reduction potential (ORP) were calculated [20]. The secondary system temperature was fixed at 270 ^{o}C, and the same water chemistry condition as this experiment and flowing option were used. In Fig. 7, the ECP measurement results at ΔT=25 ^{o}C were compared with the MULTEQ® prediction results. The measurement results showed similar behaviors compared with the prediction results by MULTEQ® although the absolute values showed some discrepancy.

Packed Crevice

To simulate fouling crevice with sludge or impurities, the experiment was repeated with a magnetite-packed crevice. Magnetite particle prior to the introduction had a mean particle size of 40 μm. The porosity in the packed crevice could not be measured. Fig. 8 shows temperature variation results as a function of time at ΔT=15 ^{o}C. In this case, the region including 'TC #3', 'TC #4', 'TC #5' could be designated as wet and dry region where concentration takes place well. The region including 'TC #1' and 'TC #2' were located below the saturation temperature at an initial boiling state. But about 3 hours later, temperature increased gradually and showed steady states at 270 ^{o}C. The apparent concentration process observed from the boiling point elevation can be attributed to a steep temperature gradient across the gap such that the tube OD surface is at above the saturation temperature but the location of temperature measurement is at under the saturation. As concentration takes place, the temperature profile across the gap will be changed and the measurement temperature also will be affected. As shown in Fig. 8, the temperature reached a steady state about 7 hours later after boiling occurred. ΔT_p also was shown but there was no significant change between prior and posterior to crevice boiling. When boiling was suppressed by increasing the pressure, the temperature returned to an initial value.

Fig. 9 shows temperature and ECP variation results as a function of time for the same condition as Fig. 8. Bulk ECP showed very stable behavior and the ECP in boiling condition was slightly lower than the ECP in non-boiling condition. This is probably because the temperature of bulk solution increases when boiling occurs. Crevice ECP was maintained at about -860 mV_{SHE} before boiling. After boiling, crevice ECP decreased with some fluctuation down to about –1050 mV_{SHE}. But the ECP could not be measured continuously due to the loss of electric path by boiling. Shortly after the boiling was discontinued, crevice ECP showed -

980 mV_{SHE} and then ECP increased gradually but did not return to the initial value. It was interpreted that under the packed crevice condition the mass transport was restricted and some of the sodium ions concentrated by boiling process diffused out but some remained in crevice. The cause of the deviation of the potential recovery that was also observed in the open crevice is not clear. The difference between the initial crevice ECP and the lowest ECP was about 190 mV. Assuming that the boiling point elevation was about 6 ^{o}C at the middle-crevice, MULTEQ® predicted result was about 160 mV that agrees with the experimental results within the error range of the electrode.

Fig. 10 shows the temperature variation results as a function of time at ΔT=20 ^{o}C. Shortly after boiling occurred, the crevice temperature dropped, which was a usual phenomenon through these crevice boiling experiment, and sprang up immediately. It was interpreted that the vaporization of crevice solution decreased the crevice temperature initially and steam was superheated because liquid could not penetrate into the packed crevice. The temperature of 'TC #1' dropped to 268 ^{o}C and in this case the secondary saturation temperature was considered as 268 ^{o}C. From the measurement data, it could be concluded that the bottom region of crevice was filled with steam initially but the concentrated liquid region located at the middle of crevice expanded to the crevice bottom and the upper region.

Fig. 11 shows the temperature and ECP variation results as a function of time at ΔT=20 ^{o}C. Because this experiment was conducted after the case of ΔT=15 ^{o}C, the initial crevice ECP showed a very low potential. Under the boiling condition, the crevice ECP showed a slightly lower value than that of non-boiling condition. When the boiling was suppressed, the crevice ECP had a stable value at -870 mV_{SHE}. The cause of different ECP behavior from other results may be the effect of magnetite particles that convert to other element, such as $HFeO_2^-$ and acidify the crevice solution.

Fig. 12 shows the axial temperature profiles with variation of primary water temperature at the condition of packed crevice compared with the case of open crevice. Except the case of 280 ^{o}C, the temperature in crevice region for the packed crevice is about 2 ^{o}C higher than the one for the open crevice. In the case of 280 ^{o}C, the temperature at shallow crevice is higher than deep crevice. This may be the result of very short liquid penetration depth in the packed crevice that can facilitate easier concentration process. Packed crevice also had much longer time to get steady states and showed heavier concentration than open crevice as shown in Fig. 13.

4. CONCLUSIONS

(1) To simulate a real situation of SG tubesheet crevice, HT/HP crevice simulation loop was constructed.
(2) Na concentration process in an open tubesheet crevice was confirmed from the temperature and ECP measurement data.
(3) It was observed from the temperature measurement results that the liquid penetration depth was decreased and the dry region expanded as ΔT increased. Via the concentration process the wetted region developed from the bottom of crevice.
(4) To analyze the open crevice boiling regions analytically, liquid penetration depth model was introduced. The model results estimated the liquid penetration depth more conservatively

than the measurement results.
(5) From the boiling point elevation data, the chemical concentration factor of 0.15 mm open tubesheet crevice was estimated as about 1000 for $\Delta T=25\ ^{o}C$ in the case of 50 ppm Na solution. As ΔT increased, the temperature gradient in crevice and time constant for concentration process also increased.
(6) By using MULTEQ-REDOX® Ver.2.22, high temperature solution pH, boiling point elevation, and ORP were calculated. Experimental results for open crevice showed similar behaviors compared with calculated results by MULTEQ®.
(7) The temperature in crevice region for the packed crevice was about 2 ^{o}C higher than the one for the open crevice. And in the same condition, packed crevice had much longer time to get steady states and showed heavier concentration than open crevice.
(8) As future work, direct solution sampling from crevice or the multi-measurement of ECP with crevice depth can be suggested.

ACKNOWLEDGEMENTS

This work is financially supported by the Korea Atomic Energy Research Institute (KAERI) and the National Research Laboratory Program through the Korea Institute of Science & Technology Evaluation and Planning (KISTEP).

REFERENCES

1. D. R. Diercks, W. J. Shack, J. Muscara, Nucl. Eng. Design 194 (1999): pp. 19-30.
2. Benjamin L. Dow Jr., R. C. Thomas, Nucl. Eng. Int. 43 (1998): pp. 38-40.
3. “PWR Secondary Water Chemistry Guidelines-Revision 3,” EPRI TR-102134s Rev.3 (Palo Alto, CA: EPRI, 1993).
4. “PWR Molar Ratio Control Application Guidelines, Volume 1: Summary,” EPRI TR-104811-V1 (Palo Alto, CA: EPRI, 1995).
5. J. B. Lumsden, G. A. Pollock, P. J. Stocker, P. J. Millett, C. Fauchon, "Hideout in Prototypic Tube/Tube Support Plate Heated Crevices," Proc. 8th Int. Symp. Environmental Degradation of Materials in Nuclear Power Systems-Water Reactors (Amelia Island, FL: American Nuclear Society, 1997), p. 108.
6. A. J. Baum, "Restricted Geometries and Deposits," The ASME Handbook on Water Technology For Thermal Power Systems, ed. P. Cohen (New York, NY: The American Society of Mechanical Engineers, 1989), Ch. 6-3.
7. Y. Kozawa, S. Aoki, "Alternate Drying and Rewetting of Heat Transfer Surface in Tubesheet Crevice," ASME Technical Paper, 82-JPGC-NE-6, 1982.
8. S. Tieszen, H. Merte, Jr., V. S. Arpaci, S. Selamoglu, ASME J. Heat Transf., 109 (1987): pp.761-767.
9. A. J. Baum, N. J. Curlee, "An Experimental and Analytical Investigation of Dryout and Chemical Concentration in Confined Geometries," ASME Technical Paper, 80-C2/NE-6, 1980.

10. J-L. Campan, C. E. Shoemaker, "Sodium Hideout Studies in Steam Generator Crevices," Proc. 3rd Int. Symp. Environmental Degradation of Materials in Nuclear Power Systems-Water Reactors (Traverse City, Michigan: The Metallurgical Society, 1987), pp. 199-207.
11. Robert E. Hermer, Richard J. Jacko, A. Kishida, H. Takamatsu, "The Measurement of Simulated Steam Generator Crevices," Proc. 3rd Int. Symp. Environmental Degradation of Materials in Nuclear Power Systems-Water Reactors (Traverse City, Michigan: The Metallurgical Society, 1987), pp. 191-198.
12. A. M. Brennenstuhl, A. McBride, D. Graham, "An Assessment of High Temperature Electrochemical Noise to Monitor the Effects of Chemical Excursions on the Corrosion Response of UNS N08800 Nuclear Steam Generator Tubes," Proc. 8th Int. Symp. Environmental Degradation of Materials in Nuclear Power Systems-Water Reactors (Amelia Island, FL: American Nuclear Society, 1997), pp. 3-10.
13. H. Takamatsu, S. Isobe, M. Sato, K. Arioka, T. Tsuruta, "Monitoring on Corrosion Behavior of Steam Generator Tubings," Proc. JAIF Int. Conf. Water Chemistry in Nuclear Power Plants-Operational Experience and New Technologies for Management (Tokyo, Japan, 1988), pp. 648-653.
14. H. Takamatsu, K. Matsueda, E. Kadokami, K. Arioka, T. Tsuruta, S. Okamoto, T. Ueno, "Evaluation of SG Crevice Environment by Directly Sampled Method Using an On-site Autoclave Facility," Proc. 5th Int. Symp. Environmental Degradation of Materials in Nuclear Power Systems-Water Reactors (Monterey, CA: American Nuclear Society, 1991), pp. 752-756.
15. T. Tsuruta, S. Okamoto, T. Kitera, H. Takamatsu, T. Matsunaga, "IGA/SCC Crack Propagation Rate Measurements on Alloy 600 SG Tubing and Evaluation of Crevice Environments Using a Side Stream Model Boiler," Proc. 7th Int. Symp. Environmental Degradation of Materials in Nuclear Power Systems-Water Reactors (Breckenridge, Colorado: NACE, 1995), pp. 187-197.
16. C. B. Bahn, S. Oh, I. S. Hwang, H. S. Chung, S. Jegarl, J. Korean Electrochem. Soc., 4 (2001): p. 87.
17. Allen Baum, “The Mechanics of Concentration Processes in Recirculating Nuclear Steam Generators,” Proc. Conf. on Water Chemistry and Corrosion in the Steam-Water Loops of Nuclear Power Stations (Seillac, France, 1980).
18. P. J. Millett, J. M. Fenton, Nucl. Tech. 108 (1994): p. 256.
19. C. B. Bahn, I. S. Hwang, I. H. Rhee, U. C. Kim, J. W. Na, “Experimental Simulation of Boiling Crevice Chemistry,” Proc. 9th Int. Symp. Environmental Degradation of Materials in Nuclear Power Systems-Water Reactors (Newport Beach, CA:TMS, 1999), pp. 537-543.
20. “MULTEQ: Equilibrium of an Electrolytic Solution With Vapor-Liquid Partitioning Volume 3: Theory Manual,” EPRI NP-5561-CCML Volume 3 (Palo Alto, CA: EPRI, 1992).

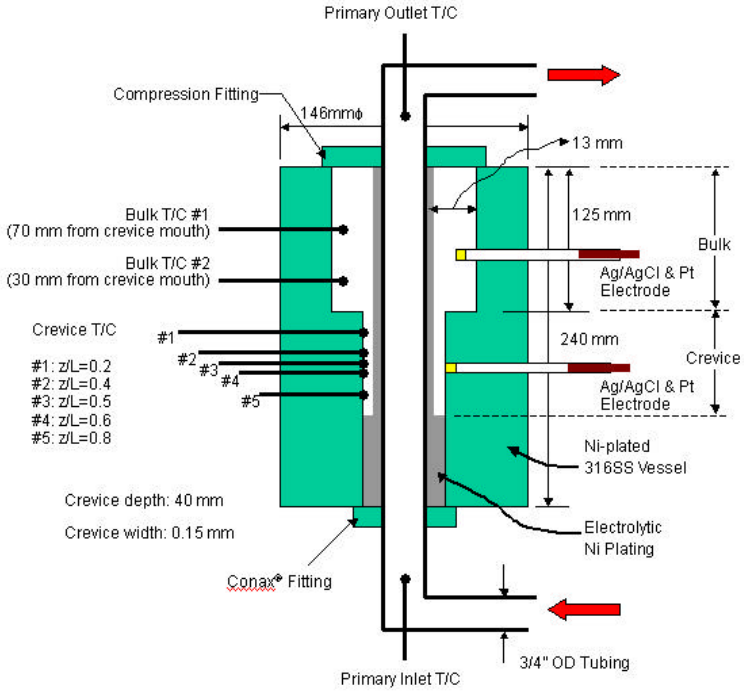

Figure 1. Schematic diagram of SG crevice simulation vessel.

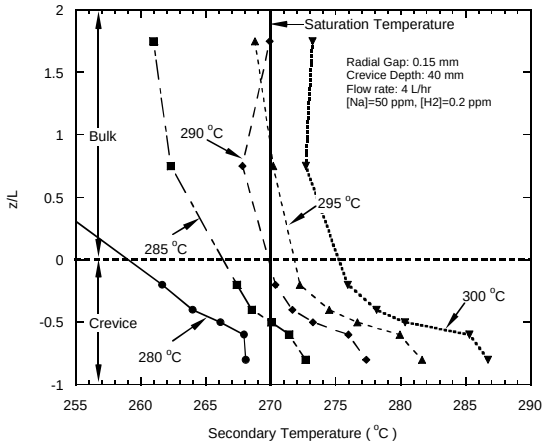

Figure 2. Axial temperature distribution in the open crevice as a function of primary water temperature.

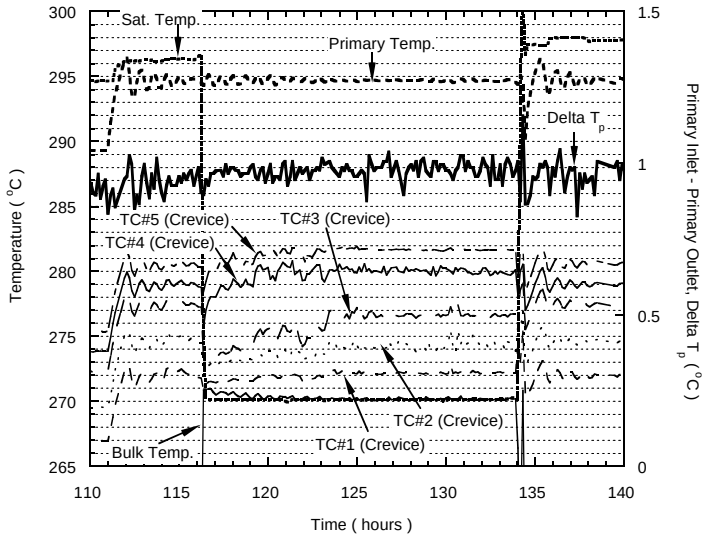

Figure 3. Temperature variation results as a function of time for open crevice with $\Delta T=25\ ^{o}C$.

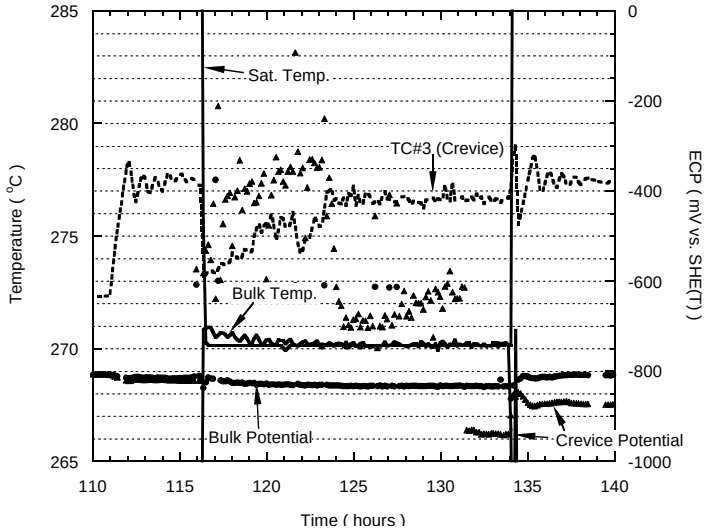

Figure 4. Temperature and ECP variation results as a function of time for open crevice with $\Delta T=25\ ^{o}C$.

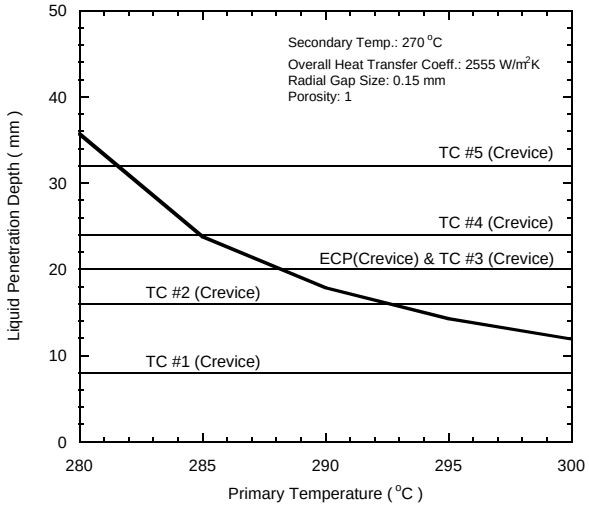

Figure 5. Liquid penetration depth prediction results for the open crevice as a function of primary water temperature.

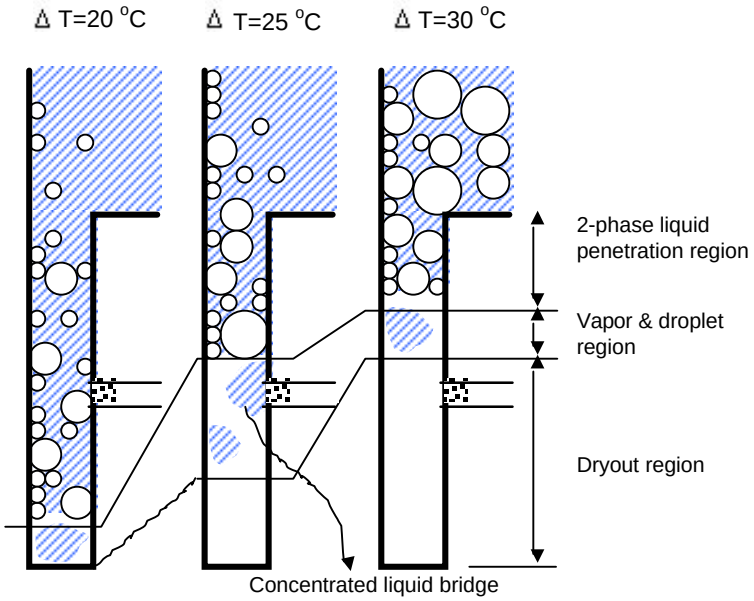

Figure 6. Schematic diagrams of crevice boiling phenomena for the open crevice as function of primary water temperature.

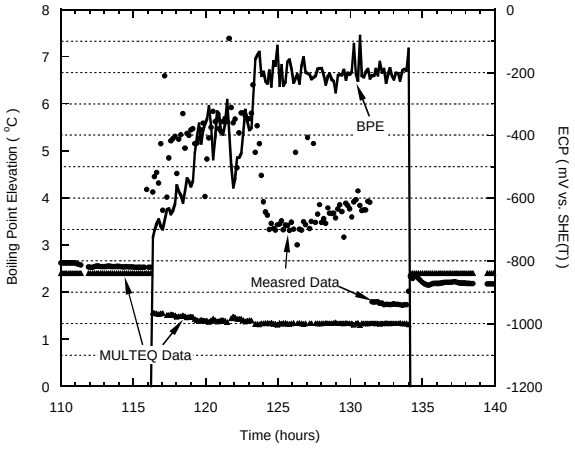

Figure 7. ECP measurement results in comparison to the MULTEQ prediction results for open crevice at $\Delta T=25\ ^{o}C$.

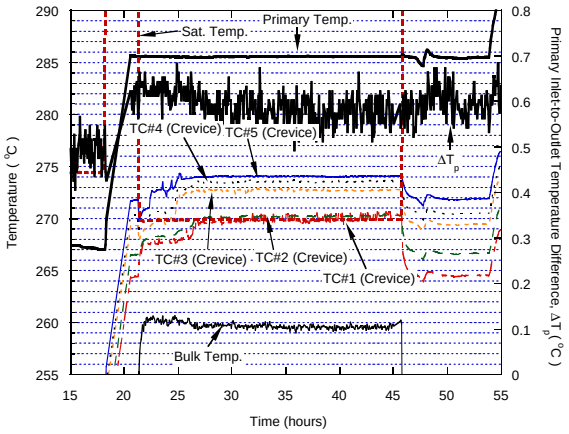

Figure 8. Temperature variation results for the packed crevice as a function of time at $\Delta T=15\ ^{o}C$.

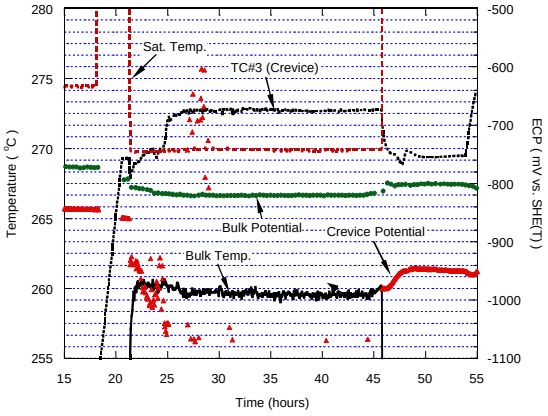

Figure 9. Temperature and ECP variation results for the packed crevice as a function of time at $\Delta T=15\ ^{o}C$.

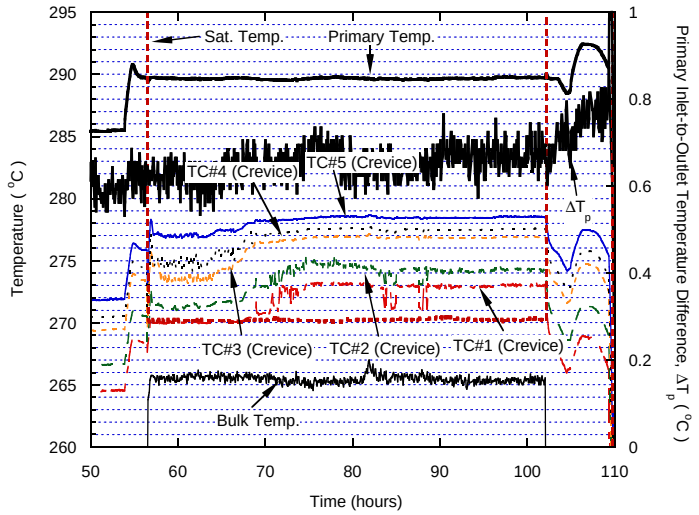

Figure 10. Temperature variation results for the packed crevice as a function of time at ΔT=20 ^{o}C.

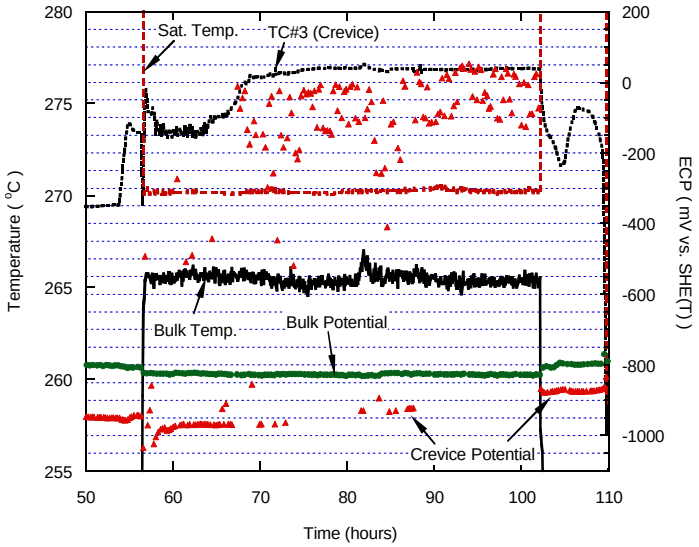

Figure 11. Temperature and ECP variation results for the packed crevice as a function of time at ΔT=20 ^{o}C.

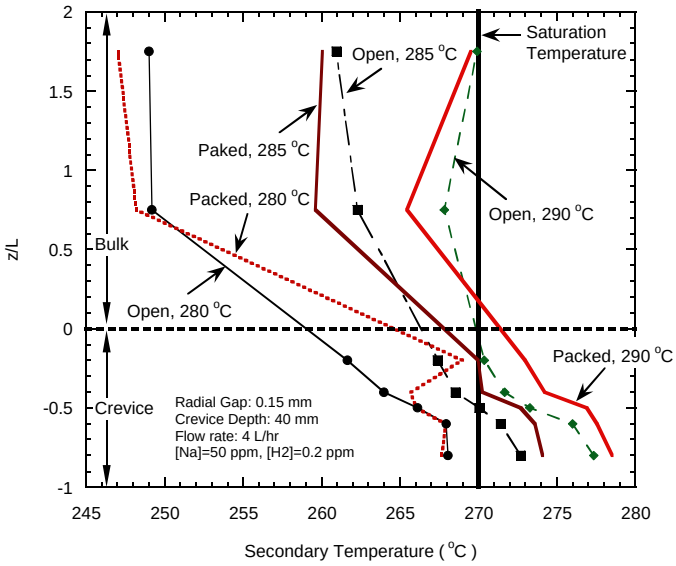

Figure 12. Comparison of the axial temperature profiles between the open crevice and the packed crevice.

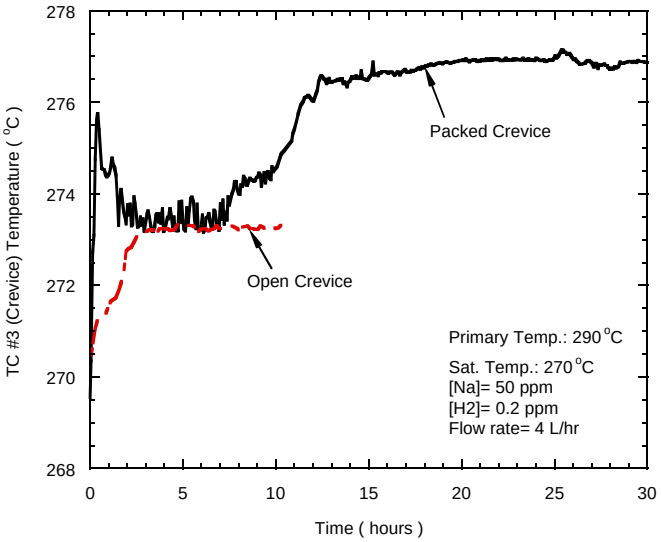

Figure 13. Comparison of the time to get a steady state between the open crevice and the packed crevice.